

Stability in Synapse Number and Size at 2 Hr after Long-Term Potentiation in Hippocampal Area CA1

Karin E. Sorra and Kristen M. Harris

Program in Neuroscience, Harvard Medical School, and Division of Neuroscience in the Department of Neurology, Children's Hospital, Boston, Massachusetts 02115

Long-term potentiation (LTP) is an important model for examining synaptic mechanisms of learning and memory. A key question is whether the enhanced synaptic transmission occurring with LTP involves the addition of new synapses, the enlargement of existing synapses, or a redistribution in synaptic weight among synapses. Two experimental designs were used to address this question. In the first experimental design three conditions were evaluated across hippocampal slices maintained *in vitro*, including slices with LTP analyzed at 2 hr post-tetanus, slices tetanized in the presence of APV, and control slices receiving test stimulation only. In the second experimental design independent LTP and control (low-frequency stimulation) sites were examined. Synapse density was estimated by an unbiased volume sampling procedure. Synapse size was computed by three-dimensional reconstruction from serial electron microscopy (EM). Serial EM also was used to compute synapse number per unit length of dendrite. In both experimen-

tal designs there were no significant effects of LTP on total synapse number, on the distribution of different types of synapses (thin, mushroom, stubby, or branched dendritic spines and macular, perforated, or segmented postsynaptic densities), on the frequency of shaft synapses, nor on the relative proportion of single or multiple synapse axonal boutons. There was also no increase in synapse size. These results suggest that LTP does not cause an overall formation of new synapses nor an enlargement of synapses at 2 hr post-tetanus in hippocampal area CA1, and these results support the hypothesis that LTP could involve a redistribution of synaptic weights among existing synapses.

Key words: long-term potentiation; hippocampus; area CA1; serial electron microscopy; dendritic spines; postsynaptic density; disector; axonal boutons; three-dimensional reconstructions; ultrastructure; hippocampal slice; *in vitro*

The cellular mechanisms for storing memory in the brain are not known, although prevailing theories include changes in synapse number or structure (Tanzi, 1893; Ramon y Cajal, 1911; Hebb, 1949; Wallace et al., 1991; Bailey and Kandel, 1993). Long-term potentiation (LTP) is an enduring enhancement of synaptic transmission that results from specific patterns of activation, occurs in many different brain regions, and is widely accepted as a cellular mechanism of learning and memory (Bliss and Lomo, 1973; Bliss and Collingridge, 1993). Hence, a useful step toward testing the structural theory of memory is to establish whether, when, and where LTP involves a change in synapse number or structure.

Considerable research has been devoted to determining whether LTP has a structural correlate (for review, see Wallace et al., 1991; Horner, 1993; Edwards, 1995). Most of the structural studies have been done in the dentate gyrus of the hippocampal formation *in vivo* and involved repeated stimulation of the perforant path input. In this region some changes in synapse number and/or structure have been reported to occur as early as 2–30 min

after induction of LTP (Van Harreveld and Fifkova, 1975; Fifkova and Van Harreveld, 1977; Fifkova et al., 1982; Desmond and Levy, 1986a,b, 1988, 1990; Trommald et al., 1990) and to have lasted for hours to days (Geinisman et al., 1991, 1994). Across the many studies, however, there are puzzling inconsistencies as to which changes are specific to LTP. Area CA1 in the hippocampal slice preparation was chosen in the present study because it has become the dominant model system for investigating the cellular and molecular bases of LTP. In previous studies single-section analyses (Lee et al., 1980; Chang and Greenough, 1984; Chang et al., 1991; Buchs and Muller, 1996) or confocal microscopy (Hosokawa et al., 1995) was used to evaluate the number or structure of hippocampal CA1 synapses after electrically or chemically induced LTP. Single-section analyses are now recognized to be inaccurate because individual synapses might be identified incorrectly or missed, and variability in synapse size, shape, or orientation substantially influences the probability of viewing them on a single section (Dubin, 1970; De Groot and Bierman, 1983; Sterio, 1984; Braendgaard and Gundersen, 1986; Coggeshall and Lekan, 1996). In addition, the irregular shapes of synapses and dendritic spines make it impossible to extrapolate from measurements made on single sections to the true three-dimensional values (Harris et al., 1992; Harris and Sultan, 1995; Spacek and Harris, 1997). Confocal microscopy does not distinguish short or curved dendritic spines from the overlapping dendritic shaft nor the occurrence of shaft synapses, and it also has insufficient resolution to measure synaptic dimensions (Harris, 1994; Trommald et al., 1995).

In the present work serial electron microscopy (EM) was used

Received July 21, 1997; revised Oct. 1, 1997; accepted Oct. 31, 1997.

This work was supported by National Institutes of Health Grants NS21184 and NS33574 (K.M.H.), MR Center Grant P30-HD18655 (Dr. Joseph Volpe, PI), the Program in Neuroscience and the Division of Medical Sciences at Harvard University, and the Natural Sciences and Engineering Research Council of Canada (K.E.S.). We thank Ms. Marcia Feinberg for expert technical assistance. We also thank Drs. John Davis and John Fiala for developing and assisting us with the reconstruction and image analysis systems in the Image Graphics Laboratory at Children's Hospital.

Correspondence should be addressed to Dr. Kristen M. Harris, Division of Neuroscience, Enders 260, Children's Hospital, 300 Longwood Avenue, Boston, MA 02115.

Copyright © 1998 Society for Neuroscience 0270-6474/98/180658-14\$05.00/0

to overcome many of these shortcomings. Unbiased sampling was achieved by a volume disector, and viewing through serial sections was used to distinguish different types of synapses. Spine numbers obtained along reconstructions of individual dendritic segments validated results from the unbiased sampling. Total postsynaptic density (PSD) area was measured as an indicator of overall synapse size because it is well correlated with the dimensions of other components of the synapse (Chicurel and Harris, 1992; Harris et al., 1992; Lisman and Harris, 1993; Sorra and Harris, 1993; Spacek and Harris, 1997). The results provide the first detailed measurements of synapse number and size in hippocampal slices and suggest that LTP does not result in synapse enlargement nor in more synapses at 2 hr post-tetanus in the mature hippocampal area CA1.

MATERIALS AND METHODS

Preparation and maintenance of hippocampal slices in vitro. Hippocampal slices were prepared from male rats of the Long-Evans strain 60–70 d old (weight 236–310 gm), according to methods adapted from (Harris and Teyler, 1984) and in accordance with National Institutes of Health guidelines and approved animal care protocols. After decapitation, the left hippocampus was removed, and four to six slices (400 μm each) were cut from the middle third of the hippocampus into ice-cold media containing (in mM) 116.4 NaCl, 5.4 KCl, 3.2 CaCl_2 , 1.6 MgSO_4 , 26.2 NaHCO_3 , 1.0 NaH_2PO_4 , and 10 D-glucose. Slices were transferred to nets positioned over wells containing media with or without 50 μM DL-amino-5-phosphonovaleric acid (APV; Sigma, St. Louis, MO) at the interface of humidified O_2 (95%) and CO_2 (5%) maintained at 30–31°C. Slices were equilibrated for at least 1 hr before physiological recordings.

Physiological recordings. Two concentric bipolar stimulating electrodes (Ultrasmall, 50 μm pole separation; Fred Haer, Brunswick, ME) were positioned 600–800 μm apart in the middle of stratum radiatum on either side of a single extracellular recording electrode (glass micropipette filled with 0.12 M NaCl; see Fig. 1a). Test stimuli consisted of alternating stimuli at each electrode delivered at one per 15 sec at an intensity that evoked field EPSPs (fEPSPs) with initial slopes measuring ~ 1 mV/msec. Increasing stimulus intensity was used to generate an input–output (*I–O*) curve, and the half-maximal responses were monitored for 20–40 min for each physiologically independent pathway before induction of LTP (see the protocols below). All responses were digitized and analyzed with Scope software (RC Electronics, Santa Barbara, CA) and converted to Lotus 1-2-3 (Lotus Development, Cambridge, MA) and Microcal Origin (Microcal Software, Northampton, MA) for subsequent analysis and graphing.

Across-slice experiments. Slices from a total of seven animals were used for these experiments. Four conditions were represented, including (1) LTP, (2) control stimulation in normal media, (3) control stimulation in media containing 50 μM APV, and (4) slices tetanized in the presence of APV (APVtet). LTP was induced by delivering tetanic stimulation (100 Hz for 1 sec at half-maximal stimulation) at both of the stimulating electrodes, either sequentially or simultaneously. Sequential tetani were separated by 10 min intervals, and pairs of simultaneous tetani were separated by 20 min intervals. Two or three sets of tetanic stimulation were delivered to ensure that LTP was saturated. Enduring LTP was defined as an increase in the initial slope of the fEPSP of at least 40% above the pretetanus value monitored for 2 hr post-tetanus (see Fig. 2a). This 2 hr time point was chosen because it is long enough after tetanus for gene induction to have occurred (Ghosh et al., 1994; Impey et al., 1996), it is in a phase of LTP that had been reported to require new protein synthesis (Otani et al., 1989; Huang and Kandel, 1994), and it is consistent with times used in other structural studies of LTP in area CA1 (Lee et al., 1980; Chang and Greenough, 1984; Chang et al., 1991; Hosokawa et al., 1995; Buchs and Muller, 1996). Control slices, with or without APV in the media, were tested with the *I–O* procedure, and their responses were monitored at the rate of one stimulus per 15 sec for 10 min at half-maximal stimulation intensity alternating between the two stimulating electrodes (Fig. 2b). Other control slices received the same tetanic stimulation protocols as the LTP slice, but in the presence of APV, which blocked LTP (APVtet, Fig. 2c). In two experiments all four conditions were obtained from four different hippocampal slices of the same animal. In other experiments an LTP and a control slice or an APVtet and an APV control slice were obtained from the same animal.

All of the results from the two control conditions that were given test stimuli only in the presence or absence of APV (conditions 2 and 3) were statistically equivalent, so these two control conditions were combined as one group (“untetanized controls,” e.g., Figs. 4, 5).

Slices from each condition were immersed in mixed aldehydes during 8 sec of microwave irradiation to ensure rapid fixation throughout the slices immediately after the physiological recordings (Jensen and Harris, 1989). Indirect lighting and a dissecting microscope were used to identify the locations of the two stimulating electrodes as depressions in the surface of stratum radiatum in area CA1. These depressions were used to guide manual trimming of the activated region from the rest of the hippocampal slice. Then the trimmed tissue piece was processed for transmission EM, and semithin (~ 1 μm) sections were cut parallel to the stimulating electrode tracks left on the surface of the slice (Fig. 1b) down to ~ 100 – 150 μm into the core of the slice. Test thin sections were evaluated by EM. Tissue preservation was judged acceptable if cell bodies, membranes, and cellular organelles (endoplasmic reticulum, mitochondria, microtubules, etc.) were intact at the ultrastructural level, and few or no dark (degenerating) processes were present in the neuropil (e.g., Fig. 3 below). A small trapezoid was centered between the two stimulating electrodes where the recording electrode had been located. The tip of the recording electrode was too small to leave a recognizable mark in the tissue, but its position had been measured relative to the two stimulating electrodes during the electrophysiological experimentation. This trapezoid was trimmed to a depth that was within the range of best tissue preservation at 100–180 μm from the air surface of the slices, and serial thin sections were cut for photomicroscopy and quantitative analyses of synapses (Fig. 1a).

Within-slice experiments. A second pair of experiments was done to evaluate synapse number and structure directly beneath the source of electrical stimulation. Two stimulating electrodes were positioned in the middle of s. radiatum, separated by ~ 600 μm with a recording electrode centered between them, as in Figure 1a. In these experiments tetanic stimulation was delivered to induce LTP at one electrode, and control low-frequency stimulation was delivered to the other electrode within the same slice. An *I–O* curve was obtained, and then the fEPSP was monitored at approximately half-maximal stimulation for at least 20 min at both sites. During the pretetanus monitor a total of three low-frequency stimulations (LFS; 5 Hz stimulation for 20 sec as two trains separated by a 20 sec interval) were delivered to the control pathway, separated by ~ 5 min each for a total of 600 pulses. At 5 min after the last LFS, tetanic stimulation (100 Hz for 1 sec as two trains separated by a 20 sec interval) was delivered via the other stimulating electrode to the LTP pathway. Additional pairs of tetanic stimulation were delivered at 10 and 20 min later to ensure that LTP was saturated (Fig. 7, below). Responses at both pathways were monitored at a rate of one stimulation every 30 sec for 2 hr post-tetanus. Input specificity was demonstrated by the occurrence of LTP from tetanic stimulation at one electrode and by no enhancement in response to stimulation at the control electrode.

In another set of experiments (data not shown) the recording electrode was positioned within 50 μm of the stimulating electrode, and the same tetanic stimulation protocol was given. These experiments demonstrated that LTP ($148\% \pm 18\%$, $n = 3$) occurs immediately adjacent to the stimulating electrode as well as centered between the two stimulating electrodes.

The exact positions of both stimulating electrodes were indicated, with respect to identifiable cellular landmarks in the slice, at the end of each physiology experiment to ensure correct identification of the LTP and control sites for subsequent anatomical analyses. Slices were fixed as described above for the across-slice experiments, and area CA1 containing the stimulating electrodes was dissected free from the surrounding tissue. A single cut was made across the depth of the slice through the middle of the stimulating electrodes, and the tissue beneath each electrode was trimmed for serial EM (Fig. 1b).

Unbiased adjustment of synaptic densities with the volume disector. These methods were extended from earlier studies (Harris et al., 1989, 1992; Harris, 1994). Using a calibrated photographic screen of the electron microscope, we divided a reference section in the middle of each series into equal fields. One of the fields was selected randomly to photograph through serial sections. All series were coded and analyzed blind as to experimental condition. Clear plastic sheets covered each micrograph so that markers could be used to number and map each synaptic complex as it was viewed through serial sections. A rectangular sampling frame was drawn on the middle reference section to contain the sampling area. Two sides of the rectangle were assigned randomly as inclusion or exclusion

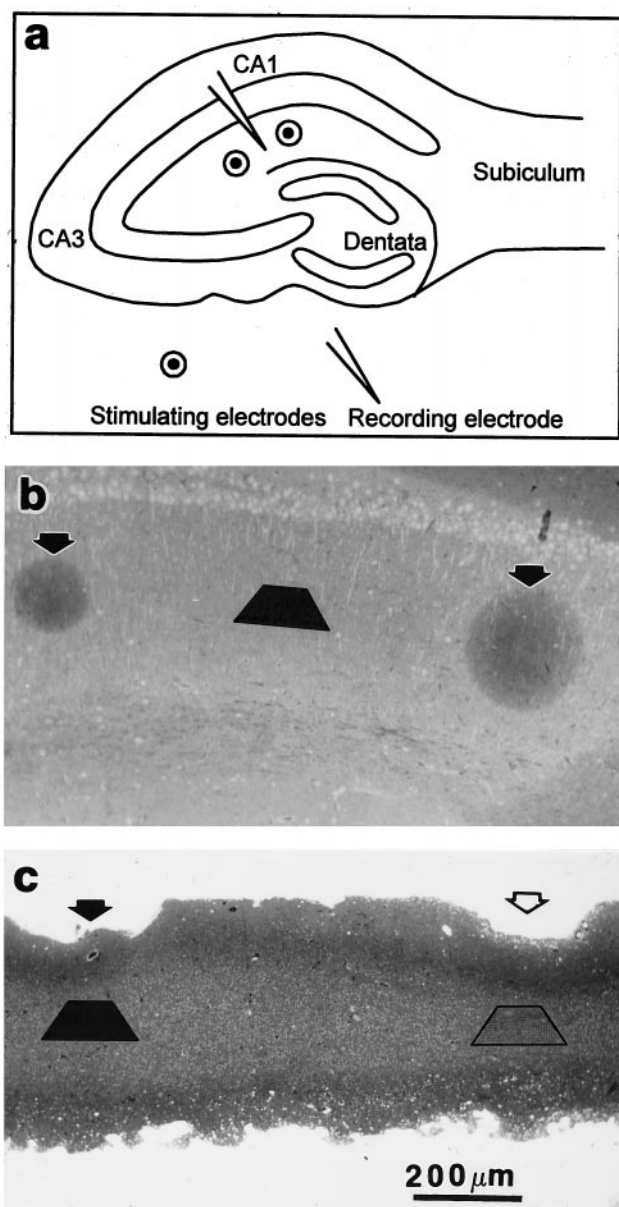


Figure 1. *a*, Schematic of electrode positions in hippocampal slices. *b*, Toluidine blue-stained section from an across-slice experiment. Sequential semithin sections ($0.5\text{--}1.0\ \mu\text{m}$) were cut parallel to the surface of the slice until the dark circles (*arrows*) created by compressed tissue beneath the tips of the stimulating electrodes disappeared. This section was located $\sim 140\ \mu\text{m}$ from the air surface of the slice. Serial thin sections were obtained between the electrodes (*black trapezoid*). *c*, Toluidine blue-stained section from a within-slice experiment. For these experiments, slices were cut across their depth from the air surface (*top*) to the net surface (*bottom*), revealing the surface depressions left by the stimulating electrodes (*arrows*). Separate sets of serial thin sections were obtained beneath the depressions left by the LTP (*filled arrow*) and control (*open arrow*) stimulating electrodes at the locations illustrated by the *black* and *stippled trapezoids*, respectively. Scale bar in *c* ($200\ \mu\text{m}$) applies to *b* and *c*.

edges to create a counting frame that minimized potential edge effects across samples (Gundersen, 1978).

To measure the sample areas, we placed the reference section from each series under a video camera and digitized it by a PC-based frame grabber (Vision-8, Insync Technologies, San Leandro, CA). The sample fields were traced and their areas computed with software entitled V8, which was developed in the Image Graphics Laboratory at Children's

Hospital. For the across-slice experiments 27 sample fields were analyzed for a total area of $3314\ \mu\text{m}^2$ ($123 \pm 20\ \mu\text{m}^2$ per sample); for the within-slice experiments 24 sample fields were analyzed for a total area of $2703\ \mu\text{m}^2$ ($113 \pm 9\ \mu\text{m}^2$ per sample). The sectioned areas of elements appearing nonuniformly in the sample field (i.e., cell bodies, large dendrites, and myelinated axons) were traced and then subtracted from the sample areas to obtain the "homogeneous neuropil area" (HNA). The total HNA was $2671\ \mu\text{m}^2$ ($99 \pm 18\ \mu\text{m}^2$ per sample) for the across-slice experiments and $2269\ \mu\text{m}^2$ ($95 \pm 9\ \mu\text{m}^2$ per sample) for the within-slice experiments.

Any PSDs falling within the sample frame or on the two inclusion lines were counted, and those falling outside of the frame or on the two exclusion lines were not counted. Synapses were always counted if the PSD and synaptic vesicles both occurred in the sample frame. PSDs sectioned *en face* or obliquely were included if the synaptic vesicles appeared in the next section. Totals of 1790 and 1438 synapses were analyzed for the across-slice and within-slice experiments, respectively. Synaptic and spine morphologies were identified as described in Results by tracing them across serial sections. One-half of the sample field in each coded series was analyzed by each author for all experiments.

PSDs have different shapes and sizes, and the probability of viewing them on the reference section differs in proportion to the number of sections they occupy. Thus, the number of serial sections each PSD occupied was counted. When the synapses were grouped by different PSD morphologies, spine shapes, or bouton types, the mean number of sections for PSDs in each category was computed. The probability of viewing different synaptic elements also varies with section thickness. Every effort was made to obtain uniform section thickness at the time of cutting (platinum-colored sections in the boat of the diamond knife); however, uniform section colors do not necessarily translate into uniform section thickness (Peachey, 1958). To correct for this potential bias, we estimated section thickness for each series by measuring the diameters of longitudinally sectioned mitochondria. The number of serial sections each mitochondrion appeared in was counted, and section thickness was estimated as thickness ($\mu\text{m}/\text{section}$) equaled measured diameter per number of sections (Harris and Stevens, 1988, 1989; Harris, 1994). Five to twenty mitochondria were included in each series to obtain this estimate of section thickness. The biased synapse density (BSD) equaled the number of synapses per HNA $\cdot 100$. Then this value was adjusted to account for the probability of viewing synapses of different shapes and sizes and for differences in section thickness. The adjusted synapse density (ASD) was the number of synapses/ $100\ \mu\text{m}^3 = \text{BSD} \cdot (1/\text{mean number of sections per PSD}) \cdot (1/\text{mean section thickness})$.

Three-dimensional reconstructions. The surface areas of PSDs were reconstructed and measured through serial sections, using the PC-based reconstruction software (V8) developed in the Image Graphics Laboratory at Children's Hospital. EM micrographs were digitized, and the images of adjacent sections were microaligned for reconstruction by flickering between the stored image and the live image and moving the live image to minimize motion of the profiles in the field. The area of cross-sectioned PSDs equaled PSD length on adjacent sections multiplied by section thickness and added across sections. For *en face* PSDs the enclosed areas were measured, and a connector was drawn to estimate where the areas overlapped in adjacent sections; the total area equaled the enclosed area plus the length of each connector multiplied by section thickness.

Statistical analysis. Lotus-1-2-3 (Lotus) was used to organize the database and to compute quantitative analyses on synapse densities. Microcal Origin (Microcal) and Statistica software (StatSoft, Tulsa, OK) were used to graph, to obtain means and SDs, to test for normality, and to perform the tests of significance described in Results. Nonparametric analyses were used for the across-slice experiments, because the data failed to approximate normal distributions as revealed with the Shapiro-Wilks' *W* test. The distribution-free Kruskal-Wallis ANOVA by ranks (where $k > 2$) and Mann-Whitney *U* (where $k = 2$) tests were used to evaluate the significance of differences between sample populations. A two-factor ANOVA was used for the within-slice experiments. The significance criterion was set at $p < 0.05$.

RESULTS

Across-slice comparisons

Physiological responses from a typical set of across-slices experiments are illustrated in Figure 2. For the LTP slices (e.g., Fig. 2*a*), the fEPSPs were potentiated at 2 hr post-tetanus, with the

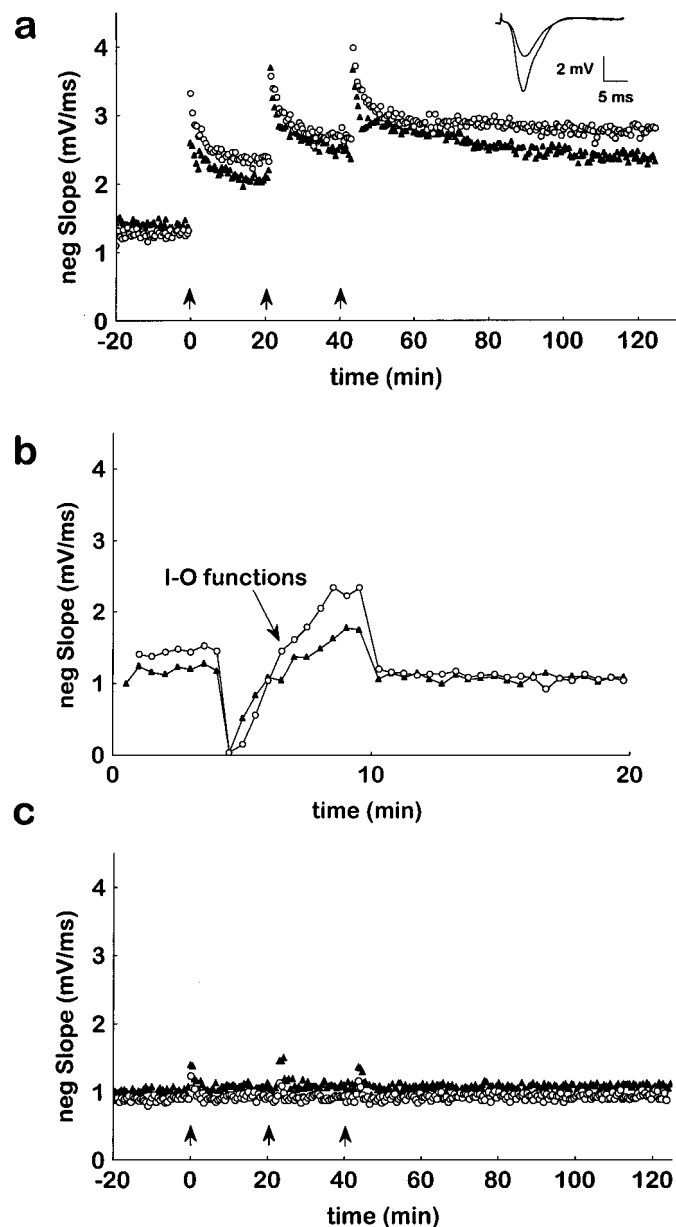


Figure 2. Representative fEPSP slopes obtained during across-slice experiments. *a*, LTP induced simultaneously in two pathways in stratum radiatum of area CA1 (open circles and filled triangles distinguish the two sets of responses). Waveforms illustrate typical pre- and 2 hr post-tetanus responses from this experiment (pretetanus is the smaller response waveform). *b*, Untetanzied slices were tested with an input–output (*I–O*) function to assess slice health and excitability at the two pathways. *c*, LTP was blocked in the presence of 50 μ M APV; arrows indicate brief post-tetanic potentiation after tetanus.

change in slope mean \pm SD = $190 \pm 40\%$ relative to the pretetanus baseline responses ($n = 6$ slices from six different animals). Untetanzied control slices ($n = 6$ slices in control media and three slices in APV containing media from seven different animals; Fig. 2*b*) achieved maximal fEPSP slopes of 2.9 ± 1.3 mV/msec, which was comparable to the pretetanus maximal fEPSP slopes of 2.9 ± 0.64 mV/msec for the LTP slices. Slices tetanzied in the presence of 50 μ M APV (Fig. 2*c*) showed no change in response ($95 \pm 10\%$, $n = 3$ slices from three different animals,

which were the same as some of the animals used for the LTP and control slices, as discussed in Materials and Methods).

Synapses were evaluated in one to three series from each of the slices for a total of 25 EM series, including 10 series from LTP slices (20–62 sections per series), 10 series (25–58 sections per series) from untetanzied control slices maintained without ($n = 6$) or with APV ($n = 3$), and 5 series (25–47 sections per series) from the three slices that were tetanzied in the presence of APV. Representative examples of the slice neuropil and synapses in each of the three treatment conditions are illustrated in Figure 3. Individual synapses were identified as macular if the PSD profiles were continuous or as perforated if electron-lucent regions divided the PSD on adjacent serial sections.

The total synapse densities were not significantly different among the LTP, the untetanzied, and the APV conditions (Fig. 4*a*). Macular synapses predominated across all three conditions (Fig. 4*b*) although only $\sim 10\%$ of the synapses were perforated. When macular and perforated synapses were analyzed separately, no significant differences were found across the treatment conditions for either type of synapse.

The dendritic spines associated with the reference section PSDs were viewed through serial sections and subjectively classified into four shape categories: thin, mushroom, stubby, and branched (Peters and Kaiserman-Abramof, 1970; Harris et al., 1992). Spines were classified as thin if their lengths were greater than their neck and head diameters; mushroom, if the heads were much wider than the necks; stubby, if the neck diameters were similar to total length; and branched, if the spines possessed more than one head. On average, 8% of the spines fell on the borders, especially between thin and mushroom shapes, and these were assigned equally to the two categories. LTP had no significant effect on the distribution of dendritic spines in these different shape categories (Fig. 5*a*).

Presynaptic boutons were identified as single synapse boutons (SSBs) if they synapsed with only one postsynaptic target and as multiple synapse boutons (MSBs) if they synapsed with two or more targets (Sorra and Harris, 1993). No differences were found across the three conditions in the frequencies of these different bouton types (Fig. 5*b*), suggesting that the number of connections between individual boutons and their postsynaptic targets was not altered by the LTP.

Shaft synapses were identified as asymmetric (excitatory) or symmetric (inhibitory) and as occurring on the spiny pyramidal cell dendrites or the nonspiny dendrites of local interneurons (Harris and Landis, 1986; Peters et al., 1991) (Figure 6). In Figure 5*a* all types of shaft synapses are combined; on average, their overall frequency is $<5\%$ of all synapses in the neuropil. Spiny dendrites predominated in all of the samples; however, the occasional nonspiny dendrite could add a disproportionate number of asymmetric shaft synapses. Because each type of shaft synapse has a distinctly different function and/or location, it was important to analyze them separately with respect to the experimental conditions. No significant differences in the frequencies of the different types of shaft synapses (asymmetric or symmetric) on either dendrite type (spiny or nonspiny) were detected (Table 1).

Within-slice comparisons

The results from the across-slice experiments showed no statistically significant differences in a variety of measurements of synapse number among the three treatment conditions. However, there appeared to be a trend toward fewer synapses in the two control conditions. To address whether variability in the data

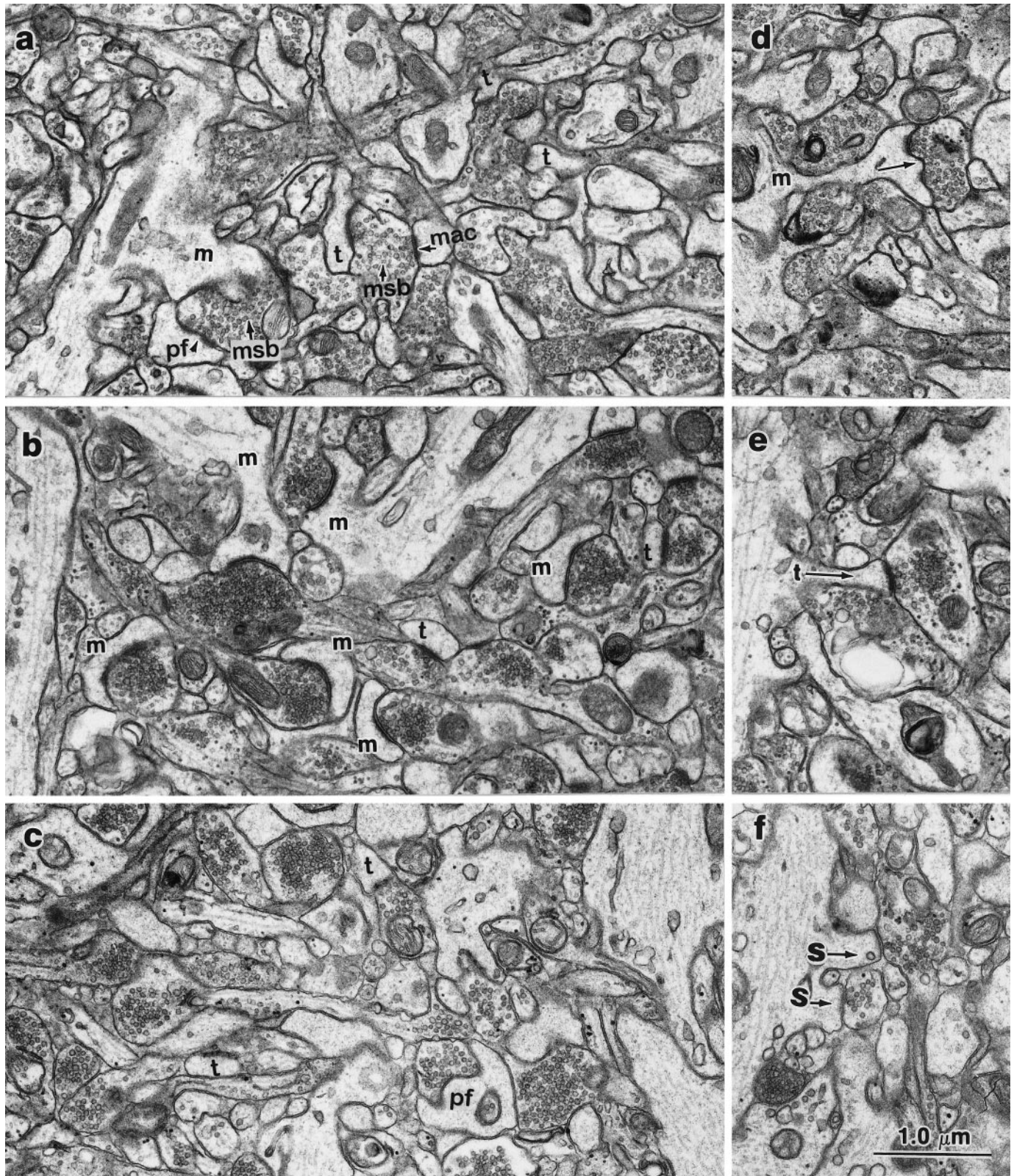


Figure 3. Ultrastructure of neuropil and synapses in *s. radiatum* of hippocampal slices from the across-slice experiments. These images were picked to illustrate the wide range in synapse density across all conditions. *a*, Region from an LTP slice; physiology of this slice is shown in Figure 2*a*. *b*, Region from an untetanized control slice; physiology is shown in Figure 2*b*. *c*, Region from a slice tetanized in the presence of APV; physiology is shown in Figure 2*c*. *d*, Longitudinal section through a mushroom-shaped dendritic spine with a perforated PSD (arrow). Portions of other mushroom spines are labeled *m* in *a*–*c*, and other perforated PSDs are labeled *pf* in *a* and *c*. *e*, Longitudinal section through a thin spine with a macular PSD (arrow). Other thin spines are labeled *t* in *a* through *c*, and a macular PSD is labeled *mac* on a multiple synapse bouton (*msb*) in *a*. A second *msb* can be seen in *a* between two mushroom spines with perforated PSDs. *f*, Longitudinal section through two neighboring stubby spines, which were relatively rare in all conditions. Scale bar in *f* applies to *a*–*f*.

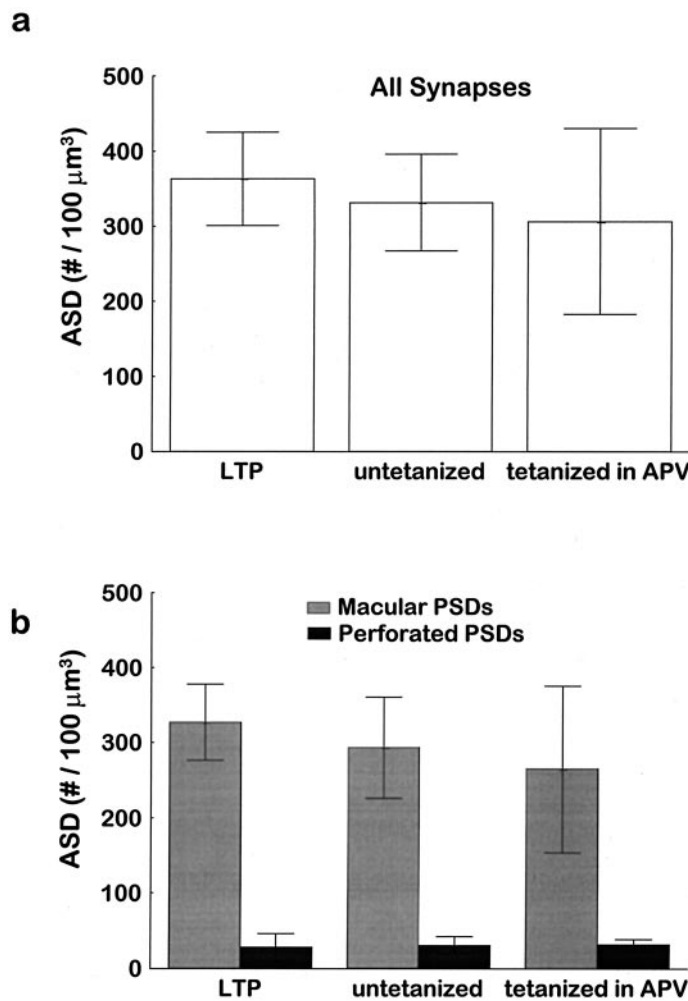


Figure 4. Synapse density and PSD morphology in hippocampal slices from the across-slice experiments. *a*, Mean-adjusted synaptic densities (ASD) \pm SD [$n = 10$ series from six slices with LTP; $n = 10$ series from nine untetanzied slices (six slices without or three slices with APV), and $n = 5$ series from three slices for the APVtet condition]. The Kruskal–Wallis ANOVA by ranks revealed no significant difference ($p = 0.17$) across these three conditions. *b*, Although macular synapses predominated in all conditions, the frequency of both macular ($p = 0.21$) and perforated synapses ($p = 0.98$) did not differ significantly across the three conditions.

masked an underlying effect of LTP on synapse number, we did a new set of experiments. These within-slice experiments were designed to minimize the variation across slices from the same and from different animals. To achieve this goal, we took advantage of the well characterized phenomenon of input specificity of LTP, wherein LTP can be induced at one stimulating electrode while low-frequency stimulation at a control site in the same slice results either in no change in response or a contrasting depression in response.

In this way, a pair of within-slice experiments (named for rat numbers 68 and 69) was performed to sample a concentrated population of LTP (i.e., potentiated) synapses beneath one stimulating electrode and nonpotentiated synapses beneath another control stimulating electrode. The neuropil was sampled directly beneath the sources of electrical stimulation at the LTP and control sites (see Fig. 1*a,c* for electrode positioning). Physiological responses from both experiments are shown in Figure 7, and representative electron micrographs are illustrated in Figure 8.

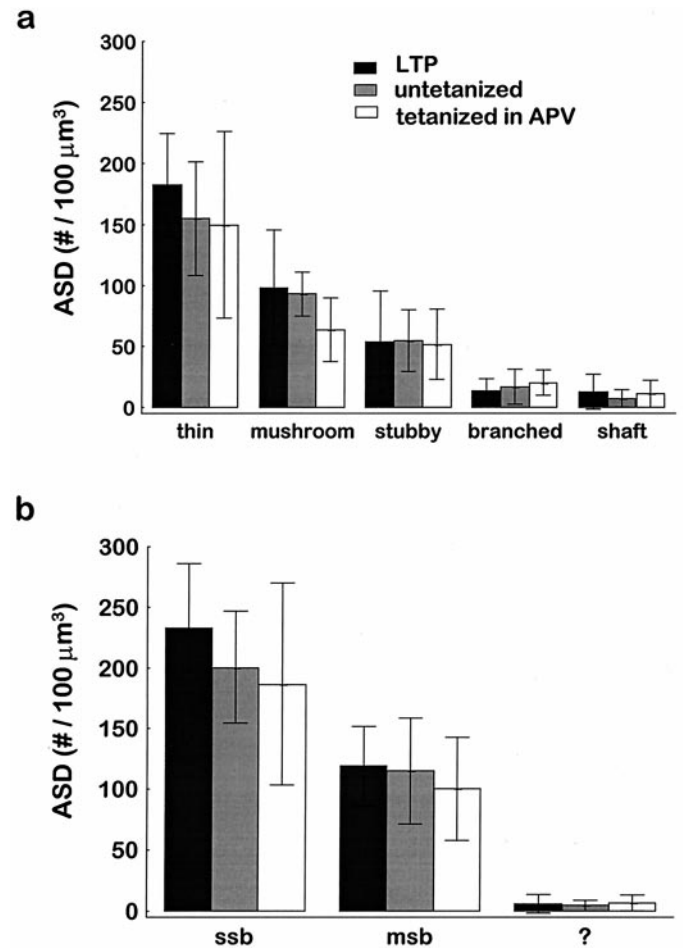


Figure 5. Quantification of dendritic spines and presynaptic boutons in the across-slice experiments. *a*, The frequencies of different types of spines were stable across all three conditions; spine types: thin spines ($p = 0.30$), mushroom spines ($p = 0.14$), stubby spines ($p = 0.75$), or branched spines ($p = 0.11$). Synapses occurring directly on dendritic shafts were rare in all of the series, with no significant differences across treatment conditions ($p = 0.93$; see also Table 1). *b*, The incidence of either single synapse boutons (ssb; $p = 0.50$) or multiple synapse boutons (msb; $p = 0.34$) did not differ across the three conditions. ? category indicates the number of boutons that could not be identified as either ssbs or msbs because they were incomplete within the series.

The physiological and anatomical data from each slice were graphed separately to control for across-animal differences. A total of 24 EM series (25–38 sections) were photographed, with six series from each slice at each of the LTP and control sites (i.e., 2 slices, 2 animals, 12 LTP series, 12 control series). This approach controlled for differences between animals and/or slices and for the amount of time a particular slice spent *in vitro* before fixation. In the within-slice experiments there were no significant differences between the LTP and control sites in the total synapse densities (Fig. 9*a*). Similarly, there were no differences in the relative frequencies of macular or perforated PSDs (Fig. 9*b*) or in the different types of shaft synapses (Table 1, within-slice experiments). There was, however, a significant difference between animals: the slice from rat 69 had a higher synapse density than rat 68 at both the LTP and control sites ($p < 0.01$).

Synapse number along individual dendritic segments

The ASD calculation, like all density estimates, could be influenced by differential growth or proliferation of other cellular

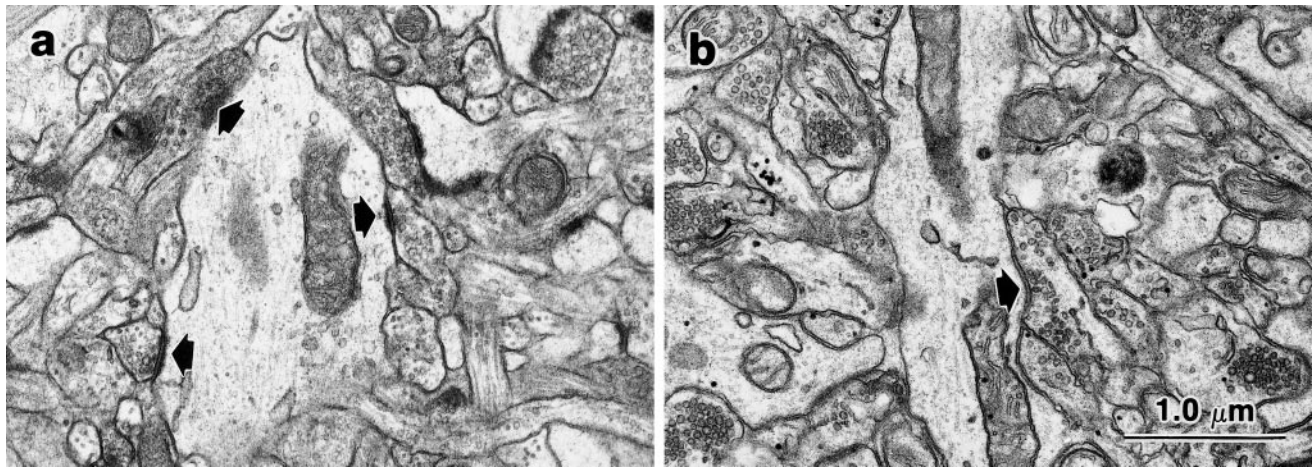


Figure 6. Ultrastructure of dendritic shaft synapses in s. radiatum of area CA1 in hippocampal slices. *a*, Asymmetric synapses (arrows) on a nonspiny dendritic shaft of an inhibitory interneuron. *b*, Symmetric synapse (arrow) identified by equal pre- and postsynaptic thickening and pleomorphic (flat and round, small and large) vesicles in the presynaptic axon. This symmetric synapse is located on a spiny dendritic shaft of a CA1 pyramidal cell.

Table 1. Occurrence of asymmetric (presumed excitatory) and symmetric (presumed inhibitory) shaft synapses on spiny and nonspiny dendrites

	LTP	Control	APVtet	<i>p</i> value
Across-slice experiments:				
Spiny dendrites:				
Asymmetric synapses	4.2 ± 4.3	2.8 ± 4.8	4.6 ± 3.9	0.34
Symmetric synapses	2.6 ± 3.8	0.5 ± 1.0	2.2 ± 2.0	0.30
Nonspiny dendrites:				
Asymmetric synapses	5.8 ± 11.6	2.0 ± 5.3	4.3 ± 8.4	0.58
Symmetric synapses	0	0	0	1
Within-slice experiments:				
Rat 68, spiny dendrites:				
Asymmetric synapses	1.4 ± 2.3	3.3 ± 2.4	—	0.20
Symmetric synapses	3.5 ± 3.8	8.6 ± 11.1	—	0.75
Nonspiny dendrites:				
Asymmetric synapses	5.0 ± 6.4	2.7 ± 4.4	—	0.58
Symmetric synapses	0.3 ± 0.6	0	—	0.63
Rat 69, spiny dendrites:				
Asymmetric synapses	6.0 ± 9.4	3.4 ± 3.6	—	1
Symmetric synapses	3.3 ± 3.0	10.0 ± 10.3	—	0.13
Nonspiny dendrites:				
Asymmetric synapses	2.1 ± 4.3	3.6 ± 4.1	—	0.63
Symmetric synapses	0.3 ± 0.8	0	—	0.63

Values are adjusted synaptic density (ASD, mean number/100 $\mu\text{m}^3 \pm \text{SD}$).

elements in the neuropil. For example, glial proliferation with LTP could lead to synapses being pushed apart in a sample volume of tissue. In fact, some evidence in the literature suggests that glial changes occur with LTP (Wenzel et al., 1991). If both synaptogenesis and glial proliferation occurred with LTP, then a change in synapse number might not be detected with the ASD calculations described above. The absolute number of spines per unit length of dendrite is a measure of synapse number that is insensitive to growth of other elements in the neuropil. This measure of synapse number could be affected by dendrites that are elongating or contracting; however, current evidence suggests that total dendritic length remains constant during LTP (Hosokawa et al., 1995; Trommald, 1995).

To compute spine number per unit length of dendrite, we identified and visually reconstructed cross-sectioned dendrites

from the LTP and control sites of the within-slice experiments across serial sections. Previous work demonstrated that the lateral thin dendrites have diameters $\leq 1 \mu\text{m}$, and the apical dendrites have diameters $>1 \mu\text{m}$ (Harris et al., 1989, 1992). Preliminary analysis from the within-slice experiments revealed that the thicker apical dendrites also had more spines per unit length (our unpublished observations), although the thinner dendrites constituted the majority. Thus, to ensure that comparable dendritic populations were sampled, only the thinner dendrites (diameters $\leq 1 \mu\text{m}$) were included here. Two hundred dendritic segments were evaluated, 50 from each of the LTP and control sites for both animals. All spines emerging from each cross-sectioned dendritic segment were counted through serial sections, and dendritic segment length was computed by multiplying the number of serial sections by section thickness. This analysis confirmed the ASD

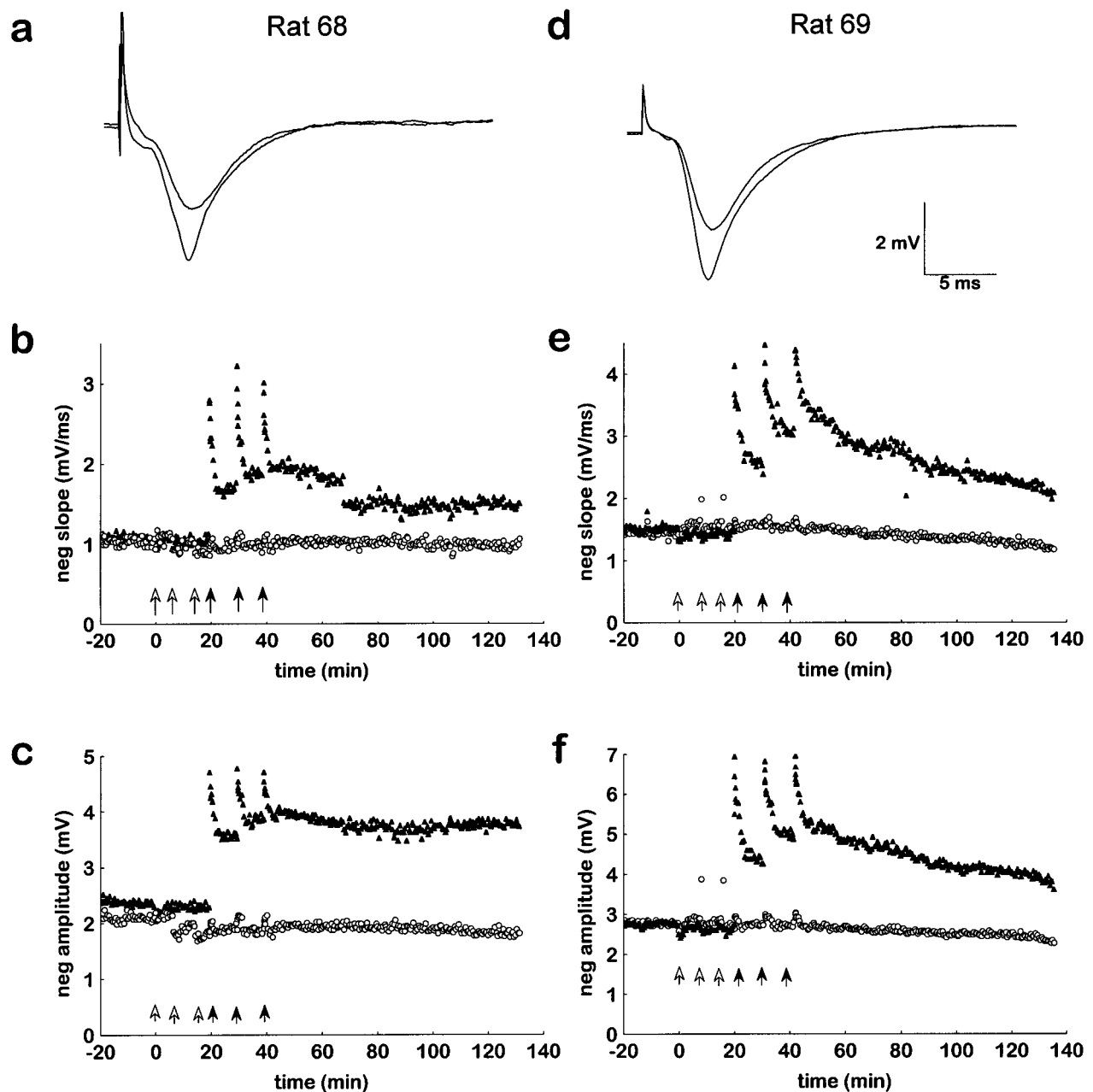


Figure 7. Summary of electrophysiological data from the two within-slice experiments: *a–c*, slices from rat 68; *d–f*, slices from rat 69. LTP was delivered to the stimulating electrode positioned in s. radiatum, closer to the CA3 side in rat 68 and closer to the subicular side in rat 69. *a, d*, Pre- and 2 hr post-tetanus waveforms; *b, e*, measured fEPSP slopes; *c, f*, amplitudes. *Open arrows* indicate where sets of low-frequency stimulation pulses were delivered to the control pathway. *Solid arrows* show where three pairs of high-frequency tetani were delivered to the LTP pathway. Slices were fixed ~2 hr after the first pair of tetani (*first filled arrow*). For rat 68, LTP was $143 \pm 5\%$ for the fEPSP slope and $165 \pm 2\%$ for the amplitude. For rat 69, LTP was $157 \pm 7\%$ for the fEPSP slope and $152 \pm 4\%$ for the amplitude. The responses at the control pathways showed no systematic change in slope or amplitude.

results reported above and showed no significant difference between the LTP and control sites in the number of dendritic spines per unit length of dendrite (Fig. 10*a*).

Branched spine analysis

Earlier studies of LTP in the hippocampal dentate gyrus provided evidence for an increased frequency of branched dendritic spines along the lengths of dendrites (Trommald et al., 1990; Trommald, 1995). To test whether branched spines were selectively affected by LTP in area CA1, we randomly selected 40 dendritic segments (10 from each of the two LTP and control sites) for a three-

dimensional analysis of the occurrence of branched spines along their lengths. Branched spines were rare along dendritic segments, and their frequency was not increased with LTP (Fig. 10*b*). There was a trend, however, toward more branched spines along dendrites at the control sites in both slices.

Synapse size

PSD area was shown previously to correlate with the size of the dendritic spine head and the amount and complexity of their subcellular constituents as well as the size of the presynaptic bouton and the number of vesicles it contains (Harris and Stevens,

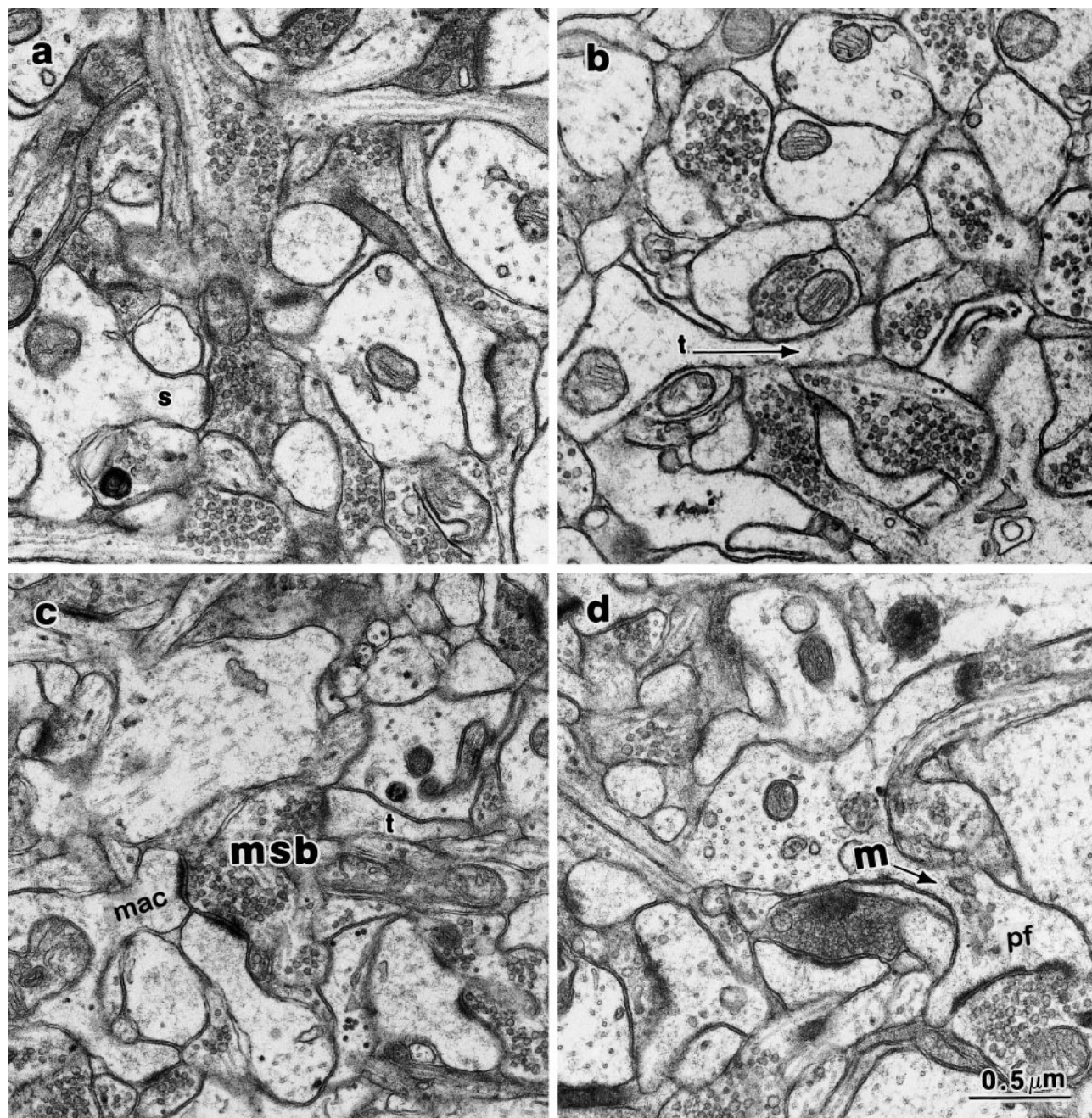


Figure 8. Electron micrographs from the within-slice experiments. *a*, LTP and (*b*) control sites from rat 68. *c*, LTP and (*d*) control sites from rat 69. In this section plane most of the dendrites are cross-sectioned, making it easier to obtain counts of dendritic spine origins than on longitudinally sectioned dendrites. Representative macular (*mac*) and perforated (*pf*) PSDs and spines of different shapes (*s*, stubby; *t*, thin; *m*, mushroom) are labeled. In addition, a typical multiple synapse bouton (*msb*) is shown in *c*. Scale bar in *d* applies to *a-d*.

1989; Harris and Sultan, 1995; Spacek and Harris, 1997). For this reason, PSD area was measured as an overall indicator of whether synapse size differed between the LTP and control sites. Sample fields from the EM series were divided into four quadrants. One or two quadrants from each series were selected randomly, and all of the PSDs contained within these quadrants were reconstructed in three dimensions. More macular than perforated synapses were reconstructed, because more macular synapses occur in area CA1 neuropil [see above and Harris et al. (1992)]. To achieve a sufficiently large population of perforated PSDs, we generated a set of random numbers, and we also reconstructed those perforated PSDs

occurring outside the reconstruction quadrant having those numbers. In total, 520 PSDs were reconstructed. These reconstructions, illustrated schematically in Figure 11*a*, revealed no differences between the LTP and control sites in the sizes of the macular PSDs (Fig. 11*b,c*) or the perforated PSDs (Fig. 11*d*), except in one slice in which the perforated PSDs were on average smaller at the LTP site ($p < 0.05$, Fig. 11*e*).

Segmented PSDs

Segmented PSDs are a subset of perforated PSDs (Fig. 11*a*). They are characterized by a single presynaptic bouton synaps-

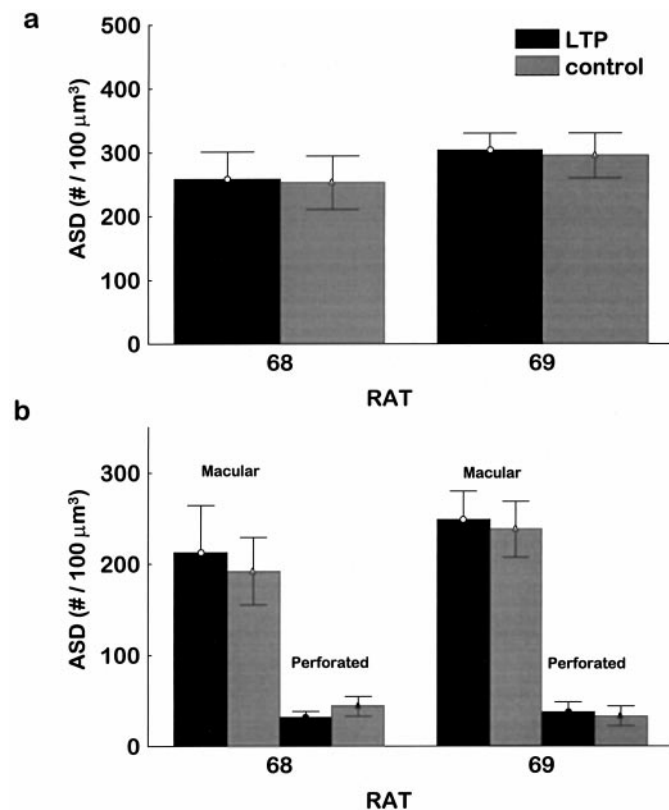


Figure 9. Adjusted synapse densities from the within-slice experiments. *a*, Total synapse density (mean \pm SD) quantified for the LTP and control sites in each of the two experiments. There was no significant difference in synapse number between the LTP and control sites for either experiment ($p = 0.63$). *b*, Macular synapses predominated in these within-slice experiments just as was shown in Figure 5*b* for the across-slice comparisons. No significant difference was observed in the incidence of macular synapses or perforated synapses between the LTP and control sites in either experiment.

ing with separate PSD areas on a single dendritic spine head (or dendritic shaft) (Geinisman et al., 1993; Harris and Sultan, 1995). In contrast, nonsegmented, perforated PSDs have electron-lucent holes in the middle of an otherwise macular PSD or are sufficiently irregular in shape that they appear perforated on some sections. A coded analysis was done of the 120 perforated PSDs that were reconstructed above to determine the relative frequencies of segmented synapses (Table 2). Only 3–27% of the perforated PSDs in these samples were fully segmented. Because the perforated PSDs are only 10% of the total synapse population (see Fig. 4*b* above), these findings indicate that only 0.3–2.7% of all synapses have segmented PSDs. There were no consistent differences in the frequency or size of segmented PSDs associated with the LTP versus control sites (Table 2).

DISCUSSION

These results suggest that LTP does not produce a change in synapse number or size at 2 hr post-tetanus in the mature hippocampal area CA1. A parsimonious interpretation is that non-structural synaptic mechanisms are sufficient to support LTP during this phase. Alternatively, concurrent synaptogenesis and synapse elimination could result in no net change in synapse number or size.

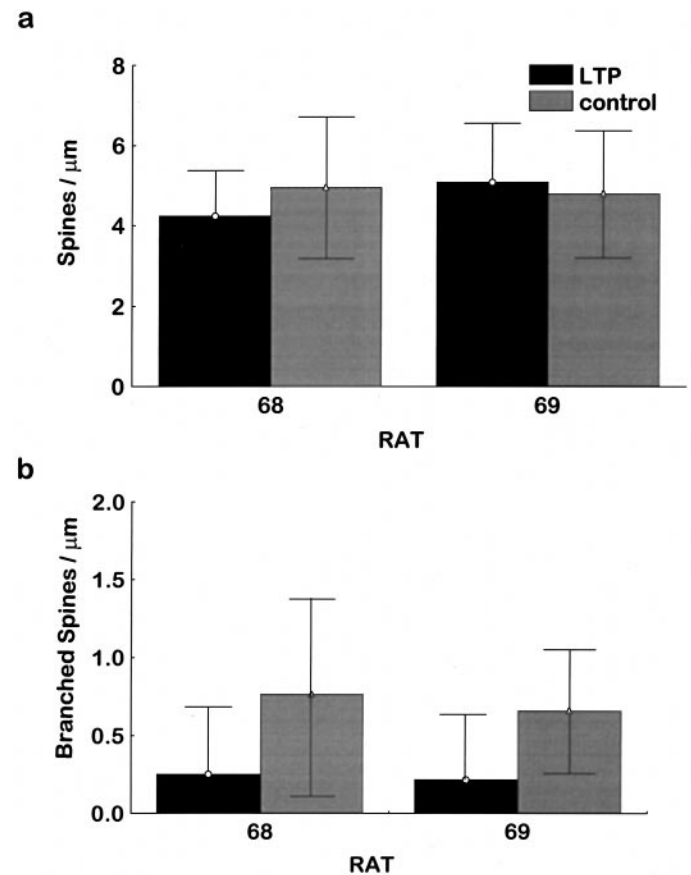


Figure 10. *a*, Spine frequencies along dendritic segments in the within-slice experiments did not differ between the LTP and control sites. *b*, Branched spines were relatively rare, and there were no significant differences in their frequencies between the LTP and control sites.

When these results are compared with those from other laboratories, several factors should be considered, including the sampling and measurement strategies, the time post-tetanus analyzed, and the experimental design. The volume disector used in this study is an unbiased procedure to adjust synaptic densities for known variables that influence sampling probability, including size, shape, and orientation of the synapse, plus the nonuniform occurrence of large and small dendrites, cell bodies, etc. The volume disector allows for inclusion of every synapse in the sampling frame, whereas other unbiased stereological approaches eliminate synapses occurring on a reference section that do not disappear on a parallel “look up” section (Gundersen, 1985; Braendgaard and Gundersen, 1986). Computation of synapse number along dendrites controls for other variables, such as growth of astrocytes, and also provides valid numbers for modeling. Finally, one of the key advantages of serial EM is that serial viewing is needed for unambiguous identification of all features of the synapse.

The main disadvantage is that serial EM is time-consuming, which makes the analysis of large numbers of samples difficult. If LTP were to have multiple forms and the anatomical effects were not always invoked, then detection of a small but significant change could require a large number of samples. Alternatively, LTP might be concentrated in a small number of synapses. We used two different approaches to address these issues. First, many slices from different animals were analyzed

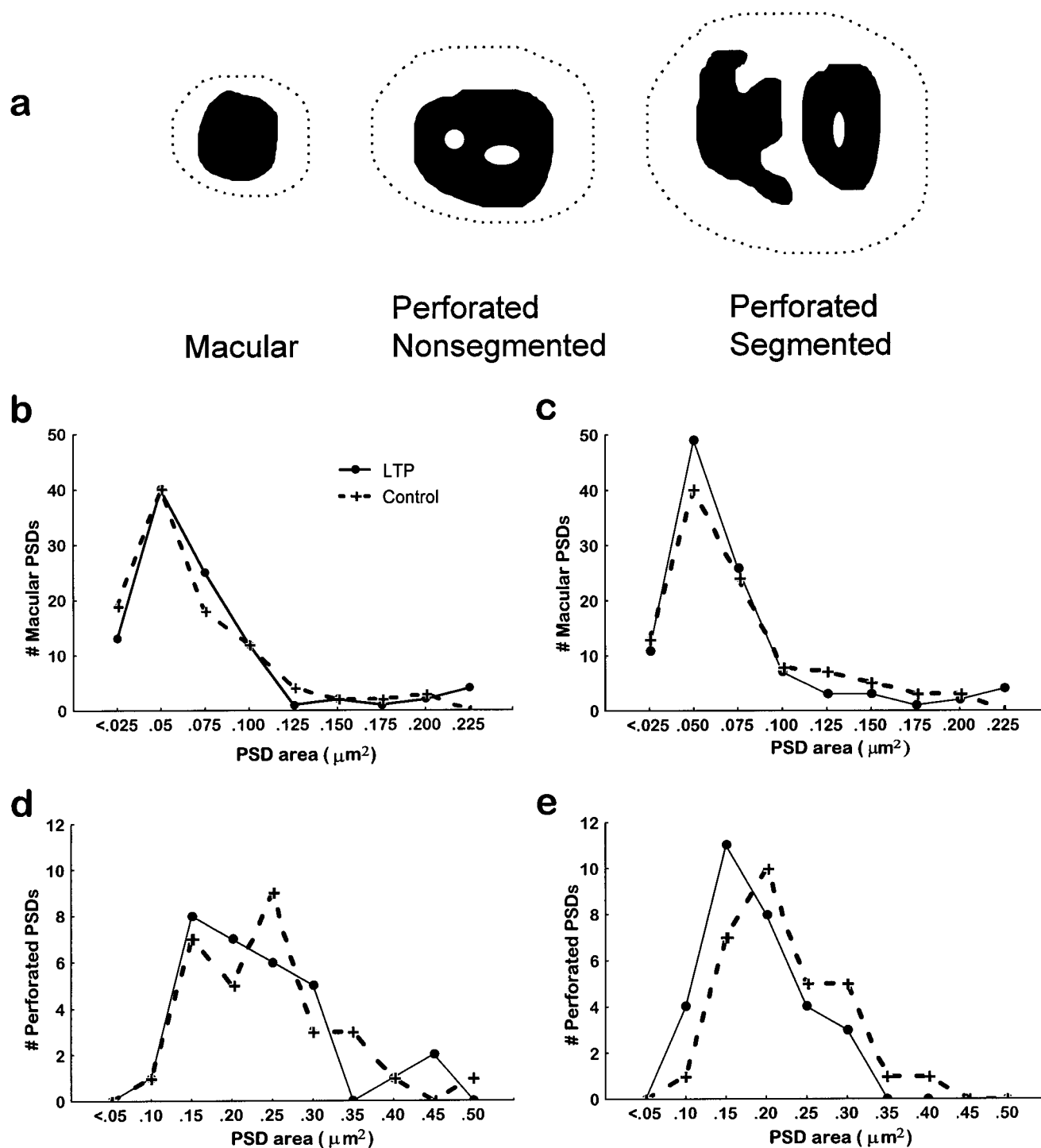


Figure 11. *a*, Schematic illustration of different types of PSDs. *b–e*, Distributions of macular and perforated PSD areas measured from the LTP (filled circles) and control (+, dashed line) sites in each of the two slices from rats 68 (*b, c*) and 69 (*d, e*). One hundred macular PSDs were measured from each LTP and control site for a total of 200 measurements per slice. No significant difference was found in the size of the macular synapses measured at the LTP versus the control sites for either rat 68 ($p = 0.49$) or rat 69 ($p = 0.67$). Perforated synapses were relatively infrequent; thus 30 perforated synapses were measured from each of the LTP and control sites in each of the two slices (total $n = 120$). Rat 68 showed no significant difference in perforated PSD size between LTP and control sites ($p = 0.53$), whereas in rat 69 the perforated PSDs measured from the control site were on average slightly larger in size than the perforated PSDs measured from the LTP site ($p = 0.036$).

in the across-slice experiments. Second, many samples were obtained in the region where the density of potentiated synapses should be highest in the two within-slice experiments. The data from the across-slice experiments were more variable

than the data from the within-slice experiments; however, the consistent findings from both experiments strengthen the basic result of no increase in overall synapse number or size at 2 hr after LTP.

Table 2. Occurrence of segmented PSDs in the within-slice experiments

	Rat 68		Rat 69	
	LTP	Control	LTP	Control
Number analyzed				
All perforated PSDs	30	30	30	30
Segmented PSDs	8	4	1	2
Percentage of perforated = segmented	27%	13%	3%	7%
Approximate percentage of total = segmented	3%	1%	0.3%	0.7%
Reconstructed PSD areas				
Nonsegmented	0.18 ± 0.05	0.19 ± 0.06	0.15 ± 0.05	0.2 ± 0.07
Segmented	0.29 ± 0.10	0.35 ± 0.07	0.28	0.13 ± 0.03

Data are presented as the number and percentages observed in the unbiased subpopulation of all perforated PSDs that were reconstructed through serial EM sections. Areas of the PSDs are expressed as mean ± SD in μm^2 .

Synapse density in the neuropil

Many other studies also have reported no change in total synapse number after LTP (Lee et al., 1980; Chang and Greenough, 1984; Desmond and Levy, 1986a,b, 1988, 1990; Gomez et al., 1990; Schuster et al., 1990; Chang et al., 1991; Geinisman et al., 1991, 1993, 1996; Grabs et al., 1991; Hosokawa et al., 1995; Buchs and Muller, 1996). However, some earlier studies in area CA1 reported a subtle but statistically significant increase in the number of stubby dendritic spines and shaft synapses, although $<2/100 \mu\text{m}^2$ were detected under all conditions (Lee et al., 1980; Chang and Greenough, 1984; Chang et al., 1991). Here we detected a higher absolute density of stubby spines and shaft synapses, but no selective effect of LTP.

Because our absolute values are higher, it seems unlikely that we missed synapses that were counted on single sections in the earlier studies (Lee et al., 1980; Chang and Greenough, 1984; Chang et al., 1991). Instead, discrepancies could result from the ambiguous identity of spine shapes on single EM sections. In the earlier studies identification was limited to spines that were sectioned longitudinally; hence fewer spines could be identified. Our higher values probably result from the reliable identification of all synapses across serial sections. For example, the heads of cross-sectioned stubby spines are often indistinguishable from the heads of mushroom spines on one section; however, the stubby spines are easily distinguished from mushroom spines with constricted necks by tracing them to their origins with the parent dendrites. Unambiguous identification is a prerequisite for unbiased and meaningful statistical comparisons between treatments (Gundersen, 1985; Braendgaard and Gundersen, 1986).

In the earlier studies from area CA1, asymmetric shaft synapses were distinguished only by the diameter of their parent dendrite (Chang and Greenough, 1984). A more explicit distinction between spiny and nonspiny dendrites is crucial, because asymmetric shaft synapses occur more frequently on the dendrites of nonspiny interneurons and both cell types have thick and thin dendrites. Asymmetric and symmetric shaft synapses also must be delineated because they are functionally distinct. The maintenance phase of LTP was analyzed recently in the dentate gyrus at 13 d after four consecutive daily periods of tetanic stimulation to the perforant pathway. The only statistically significant increase was in the asymmetric shaft synapses (Geinisman et al., 1996). Because asymmetric synapses occur more frequently on the shafts of nonspiny interneurons and these were not distinguished from the spiny granule cell dendrites, it is a possibility that the long-

term changes in the frequency of shaft synapses occurred on the nonspiny interneurons.

Spine number along individual dendrites

Trommald et al. (1990, 1995) reported increases in spine number along dendritic segments in the dentate gyrus at 30 min after tetanic stimulation of the perforant path input. Their analyses used serial EM reconstructions from two animals, along 34 and 28 dendritic segments in the control and LTP conditions, respectively. On average, there was one spine per micrometer in the control condition and three to four spines per micrometer in the LTP condition. In area CA1 we analyzed 200 dendrites, also from two different animals, and found approximately four spines per micrometer both in the control condition and in the LTP condition at 2 hr post-tetanus. It will be interesting to determine whether LTP induces more spines in area CA1 at 30 min post-tetanus, with a concomitant loss after 2 hr.

Branched spines

In the same analyses Trommald and colleagues detected a selective increase in branched dendritic spines at 30 min post-tetanus. In area CA1 we found no significant differences between the LTP and control conditions for branched spines. Branched spines composed $<5\%$ of the total spine population in the mature area CA1 (K. Sorra, J. Fiala, K. Harris, unpublished observations) and $\sim 2\%$ in the dentate gyrus (Trommald et al., 1990; Trommald, 1995). Thus, it will be valuable to increase the sample size in both regions at 30 min to determine whether spine branching provides a consistent structural basis for the early phase of LTP.

Spine shape and PSD size

Spine shape is highly irregular, and spine heads vary by >100 -fold in volume (Harris et al., 1992; Harris and Kater, 1994; Trommald and Hulleberg, 1997). The functional implications of this variation are not known; however, it is thought that the spine heads provide biochemical compartmentalization for synaptic plasticity (for review, see Harris and Kater, 1994; Koch et al., 1995; Denk et al., 1996). A spine head can appear large and indented on one section and small and convex two sections later, thereby making it difficult to interpret measurements of spine perimeters and areas on single sections (Van Harrevel and Fifkova, 1975; Lee et al., 1980; Fifkova and Andersen, 1981; Fifkova et al., 1982; Chang and Greenough, 1984; Desmond and Levy, 1988, 1990; Petit et al., 1989). We used the three-dimensional criteria of Peters and Kaiserman-Abramhoff to analyze spine shape as thin, mushroom,

or stubby because they provide a useful convention to estimate whether spine dimensions change with LTP (Harris et al., 1992). An increase in spine volume would be expressed as a shift from the stubby and thin to the mushroom shapes and vice versa. Spine shortening would be detected by a shift from thin to stubby spines, although lengthening probably would have been missed because stubby spines are so rare in the mature hippocampus. Similarly, an enlarging of existing mushroom spines would have been missed. No significant shifts among spine shapes were observed.

To examine this question further, we measured the area of the PSD, because it correlates with total spine volume, the number of docked and nondocked presynaptic vesicles, and intra-spine organelles ($r > 0.9$) (Harris and Stevens, 1989; Harris et al., 1992; Harris and Sultan, 1995; Spacek and Harris, 1997; Trommald and Hulleberg, 1997). No significant change in PSD size occurred with LTP. It is possible, however, that during the different phases of LTP other indicators of synaptic efficacy, such as vesicle number and clustering (Applegate et al., 1987; Meshul and Hopkins, 1990; Chang et al., 1991; Malgaroli et al., 1995; Ryan and Smith, 1995; Murthy et al., 1997), become disassociated from PSD size, and these deserve examination in future studies.

Segmented PSDs

Our observations suggest that segmented PSDs are not selectively affected by LTP in hippocampal area CA1. Geinisman et al. (1996, 1993, 1991) reported no change in the total synapse number or in the incidence of macular synapses after LTP in the hippocampal dentate gyrus, consistent with our findings above; however, the frequency of segmented PSDs was greater after LTP in the dentate gyrus. This discrepancy could reflect differences across brain regions or in sampling strategies.

Other work in area CA1 revealed calcium precipitates in dendritic spines with perforated PSDs at 35 min after LTP, and it was concluded that LTP caused a threefold increase in perforated PSDs (Buchs and Muller, 1996). The Ca^{2+} precipitates, however, are more likely to be detected in those spines that contain calcium-sequestering tubules of smooth endoplasmic reticulum (SER). Spacek and Harris (1997) have shown recently that only ~20% of spines with macular PSDs contain SER, whereas 100% of the spines with perforated PSDs contain SER. Thus, the analysis of Buchs and Muller (1996) was restricted mostly to large spines that already had perforated PSDs. An alternative interpretation would be that more bound calcium is sequestered in spines with SER after LTP.

Redistribution of synaptic efficacy?

Our results are consistent with the hypothesis that LTP in the mature brain results in a redistribution of synaptic weight among existing synapses. Alternatively, synapse populations could replace one another after LTP and not be detected as a shift in the overall number or size. To test these hypotheses, specific labels will be needed to distinguish recently potentiated synapses from those that were modified by past experience (Frey and Morris, 1997; Schuman, 1997) or by concurrent heterosynaptic depression (Bear and Abraham, 1996; Coussens and Teyler, 1996; Scanziani et al., 1996). Whether structural correlates of LTP can be detected will depend on whether changes in synaptic weight result in identifiable synapse-specific tags (Frey and Morris, 1997).

REFERENCES

- Applegate MD, Kerr DS, Landfield PW (1987) Redistribution of synaptic vesicles during long-term potentiation in the hippocampus. *Brain Res* 401:401–406.

- Bailey CH, Kandel ER (1993) Structural changes accompanying memory storage. *Annu Rev Physiol* 55:397–426.
- Bear MF, Abraham WC (1996) Long-term depression in hippocampus. *Annu Rev Neurosci* 19:437–462.
- Bliss TVP, Collingridge GL (1993) A synaptic model of memory: long-term potentiation in the hippocampus. *Nature* 361:31–39.
- Bliss TVP, Lomo T (1973) Long-lasting potentiation of synaptic transmission in the dentate area of the anaesthetized rabbit following stimulation of the perforant path. *J Physiol (Lond)* 232:331–356.
- Braendgaard H, Gundersen HJG (1986) The impact of recent stereological advances on quantitative studies of the nervous system. *J Neurosci Methods* 18:39–78.
- Buchs P-A, Muller D (1996) Induction of long-term potentiation is associated with major ultrastructural changes of activated synapses. *Proc Natl Acad Sci USA* 93:8040–8045.
- Chang FF, Greenough WT (1984) Transient and enduring morphological correlates of synaptic activity and efficacy change in the rat hippocampal slice. *Brain Res* 309:35–46.
- Chang FF, Isaacs KR, Greenough WT (1991) Synapse formation occurs in association with the induction of long-term potentiation in two-year-old rat hippocampus *in vitro*. *Neurobiol Aging* 12:517–522.
- Chicurel ME, Harris KM (1992) Three-dimensional analysis of the structure and composition of CA3 branched dendritic spines and their synaptic relationships with mossy fiber boutons in the rat hippocampus. *J Comp Neurol* 325:169–182.
- Coggeshall RE, Lekan HA (1996) Methods for determining numbers of cells and synapses: a case for more uniform standards of review. *J Comp Neurol* 364:6–15.
- Coussens CM, Teyler TJ (1996) Long-term potentiation induces synaptic plasticity at nontetanized adjacent synapses. *Learn Mem* 3:106–114.
- De Groot DMG, Bierman EPB (1983) The complex-shaped “perforated” synapse—a problem in quantitative stereology of the brain. *J Microsc* 131:355–360.
- Denk W, Yuste R, Svoboda K, Tank DW (1996) Imaging calcium dynamics in dendritic spines. *Curr Opin Neurobiol* 6:372–378.
- Desmond NL, Levy WB (1986a) Changes in the numerical density of synaptic contacts with long-term potentiation in the hippocampal dentate gyrus. *J Comp Neurol* 253:466–475.
- Desmond NL, Levy WB (1986b) Changes in the postsynaptic density with long-term potentiation in the dentate gyrus. *J Comp Neurol* 253:476–482.
- Desmond NL, Levy WB (1988) Synaptic interface surface area increases with long-term potentiation in the hippocampal dentate gyrus. *Brain Res* 453:308–314.
- Desmond NL, Levy WB (1990) Morphological correlates of long-term potentiation imply the modification of existing synapses, not synaptogenesis, in the hippocampal dentate gyrus. *Synapse* 5:139–143.
- Dubin MW (1970) The inner plexiform layer of the vertebrate retina: a quantitative and comparative electron microscopic analysis. *J Comp Neurol* 140:479–506.
- Edwards FA (1995) LTP—a structural model to explain the inconsistencies [comments]. *Trends Neurosci* 18:250–255.
- Fifkova E, Andersen CL (1981) Stimulation-induced changes in dimensions of stalks of dendritic spines in the dentate molecular layer. *Exp Neurol* 74:621–627.
- Fifkova E, Van Harreveld A (1977) Long-lasting morphological changes in dendritic spines of dentate granule cells following stimulation of the entorhinal area. *J Neurocytol* 6:211–230.
- Fifkova E, Anderson CL, Young SJ, Van Harreveld A (1982) Effect of anisomycin on stimulation-induced changes in dendritic spines of the dentate granule cells. *J Neurocytol* 11:183–210.
- Frey U, Morris RG (1997) Synaptic tagging and long-term potentiation [comments]. *Nature* 385:533–536.
- Geinisman Y, deToledo-Morrell L, Morrell F (1991) Induction of long-term potentiation is associated with an increase in the number of axospinous synapses with segmented postsynaptic densities. *Brain Res* 566:77–88.
- Geinisman Y, deToledo-Morrell L, Morrell F, Heller RE, Rossi M, Parshall RF (1993) Structural synaptic correlate of long-term potentiation: formation of axospinous synapses with multiple, completely partitioned transmission zones. *Hippocampus* 3:435–446.
- Geinisman Y, deToledo-Morrell L, Morrell F (1994) Comparison of structural synaptic modifications induced by long-term potentiation in the hippocampal dentate gyrus of young adult and aged rats [review]. *Ann NY Acad Sci* 747:452–466.

- Geinisman Y, deToledo-Morrell L, Morrell F, Persina IS, Beatty MA (1996) Synapse restructuring associated with the maintenance phase of hippocampal long-term potentiation. *J Comp Neurol* 368:413–423.
- Ghosh A, Ginty DD, Bading H, Greenberg ME (1994) Calcium regulation of gene expression in neuronal cells. *J Neurobiol* 25:294–303.
- Gomez RA, Pozzo Miller LD, Aoki A, Ramirez OA (1990) Long-term potentiation-induced synaptic changes in hippocampal dentate gyrus of rats with an inborn low or high learning capacity. *Brain Res* 537:293–297.
- Grabs D, Voss J, Schuster T, Wenzel J, Krug M (1991) Heterosynaptic changes in number and shape of the transmission zones of axo-spino-dendritic synapses in the central nervous system following long-term potentiation. *J Hirnforsch* 32:541–545.
- Gundersen HJ (1978) Estimators of the number of objects per area unbiased by edge effects. *Microsc Acta* 81:107–117.
- Gundersen HJG (1985) Stereology of arbitrary particles. A review of unbiased number and size estimators and the presentation of some new ones, in memory of William R. Thompson. *EM Stereol* 143:3–45.
- Harris KM (1994) Serial electron microscopy as an alternative or complement to confocal microscopy for the study of synapses and dendritic spines in the central nervous system. In: *Three-dimensional confocal microscopy: volume investigation of biological specimens* (Stevens JK, Mills LR, Trogadis JE, eds), pp 421–445. New York: Academic.
- Harris KM, Kater SB (1994) Dendritic spines: cellular specializations imparting both stability and flexibility to synaptic function. *Annu Rev Neurosci* 17:341–371.
- Harris KM, Landis DM (1986) Membrane structure at synaptic junctions in area CA1 of the rat hippocampus. *Neuroscience* 19:857–872.
- Harris KM, Stevens JK (1988) Dendritic spines of rat cerebellar Purkinje cells: serial electron microscopy with reference to their biophysical characteristics. *J Neurosci* 8:4455–4469.
- Harris KM, Stevens JK (1989) Dendritic spines of CA1 pyramidal cells in the rat hippocampus: serial electron microscopy with reference to their biophysical characteristics. *J Neurosci* 9:2982–2997.
- Harris KM, Sultan P (1995) Variation in number, location, and size of synaptic vesicles provides an anatomical basis for the non-uniform probability of release at hippocampal CA1 synapses. *J Neuropharmacol* 34:1387–1395.
- Harris KM, Teyler TJ (1984) Developmental onset of long-term potentiation in area CA1 of the rat hippocampus. *J Physiol (Lond)* 346:27–48.
- Harris KM, Jensen FE, Tsao B (1989) Ultrastructure, development, and plasticity of dendritic spine synapses in area CA1 of the rat hippocampus: extending our vision with serial electron microscopy and three-dimensional analyses. In: *The hippocampus—new vistas, neurology and neurobiology*, Vol 52 (Chan-Palay V, Kohler C, eds), pp 33–52. New York: Liss.
- Harris KM, Jensen FE, Tsao B (1992) Three-dimensional structure of dendritic spines and synapses in rat hippocampus (CA1) at postnatal day 15 and adult ages: implications for the maturation of synaptic physiology and long-term potentiation. *J Neurosci* 12:2685–2705.
- Hebb DO (1949) *Organization of behavior*. New York: Wiley.
- Horner CH (1993) Plasticity of the dendritic spine. *Prog Neurobiol* 41:281–321.
- Hosokawa T, Rusakov DA, Bliss TV, Fine A (1995) Repeated confocal imaging of individual dendritic spines in the living hippocampal slice: evidence for changes in length and orientation associated with chemically induced LTP. *J Neurosci* 15:5560–5573.
- Huang YY, Kandel ER (1994) Recruitment of long-lasting and protein kinase A-dependent long-term potentiation in the CA1 region of hippocampus requires repeated tetanization. *Learn Mem* 1:74–82.
- Impey S, Mark M, Villacres EC, Poser S, Chavkin C, Storm DR (1996) Induction of CRE-mediated gene expression by stimuli that generate long-lasting LTP in area CA1 of the hippocampus. *Neuron* 16:973–982.
- Jensen FE, Harris KM (1989) Preservation of neuronal ultrastructure in hippocampal slices using rapid microwave-enhanced fixation. *J Neurosci Methods* 29:217–230.
- Koch C, Zador A, Brown TH (1995) Dendritic spines: convergence of theory and experiment. *Science* 256:973–974.
- Lee KS, Schottler F, Oliver M, Lynch G (1980) Brief bursts of high-frequency stimulation produce two types of structural change in rat hippocampus. *J Neurophysiol* 44:247–258.
- Lisman J, Harris KM (1993) Quantal analysis and synaptic anatomy—integrating two views of hippocampal plasticity. *Trends Neurosci* 16:141–147.
- Malgaroli A, Ting AE, Wendland B, Bergamaschi A, Villa A, Tsien RW, Scheller RH (1995) Presynaptic component of long-term potentiation visualized at individual hippocampal synapses. *Science* 268:1624–1628.
- Meshul CK, Hopkins WF (1990) Presynaptic ultrastructural correlates of long-term potentiation CA1 subfield of the hippocampus. *Brain Res* 514:310–319.
- Murthy VN, Sejnowski TJ, Stevens CF (1997) Heterogeneous release properties of visualized individual hippocampal synapses. *Neuron* 18:599–612.
- Otani S, Marshall CJ, Tate WP, Goddard GV, Abraham WC (1989) Maintenance of long-term potentiation in rat dentate gyrus requires protein synthesis but not messenger RNA synthesis immediately post-tetanzation. *Neuroscience* 28:519–526.
- Peachey LD (1958) Thin sections. I. A study of section thickness and physical distortion produced during microtomy. *J Biophys Biochem Cytol* 4:233–245.
- Peters A, Kaiserman-Abramof IR (1970) The small pyramidal neuron of the rat cerebral cortex. The perikaryon, dendrites, and spines. *J Anat* 127:321–356.
- Peters A, Palay SL, Webster HD (1991) *The fine structure of the nervous system: the neurons and supporting cells*. Philadelphia: Saunders.
- Petit TL, LeBoutillier JC, Markus EJ, Milgram NW (1989) Synaptic structural plasticity following repetitive activation in the rat hippocampus. *Exp Neurol* 105:72–79.
- Ramon y Cajal S (1911) *Histologie du system nerveux de l'homme et vertebres*. Madrid: Instituto Ramon y Cajal.
- Ryan TA, Smith SJ (1995) Vesicle pool mobilization during action potential firing at hippocampal synapses. *Neuron* 14:983–989.
- Scanziani M, Malenka RC, Nicoll RA (1996) Role of intercellular interactions in heterosynaptic long-term depression. *Nature* 380:446–450.
- Schuman EM (1997) Synapse specificity and long-term information storage. *Neuron* 18:339–342.
- Schuster T, Krug M, Wenzel J (1990) Spinules in axospinous synapses of the rat dentate gyrus: changes in density following long-term potentiation. *Brain Res* 523:171–174.
- Sorra KE, Harris KM (1993) Occurrence and three-dimensional structure of multiple synapses between individual radiatum axons and their target pyramidal cells in hippocampal area CA1. *J Neurosci* 13:3736–3748.
- Spacek J, Harris KM (1997) Three-dimensional organization of smooth endoplasmic reticulum in hippocampal CA1 dendrites and dendritic spines of the immature and mature rat. *J Neurosci* 17:190–203.
- Sterio DC (1984) The unbiased estimation of number and sizes of arbitrary particles using the disector. *J Microsc* 134:127–136.
- Tanzi E (1893) I fatti e le induzioni nell'odierna istologia del sistema nervoso. *Riv Sperim Freniatria Med Leg* 19:419–472.
- Trommald M (1995) Dendritic spine changes underlying synaptic plasticity in the rat hippocampal formation. PhD thesis, University of Oslo.
- Trommald M, Hulleberg G (1997) Dimensions and density of dendritic spines from rat dentate granule cells based on reconstructions from serial electron micrographs. *J Comp Neurol* 377:15–28.
- Trommald M, Vaaland JL, Blackstad TW, Andersen P (1990) Dendritic spine changes in rat dentate granule cells associated with long-term potentiation. In: *Neurotoxicity of excitatory amino acids* (Guidotti A, Costa E, eds), pp 163–174. New York: Raven.
- Trommald M, Jensen V, Andersen P (1995) Analysis of dendritic spines in rat ca1 pyramidal cells intracellularly filled with a fluorescent dye. *J Comp Neurol* 353:260–274.
- Van Harreveld A, Fikova E (1975) Swelling of dendritic spines in the fascia dentata after stimulation of the perforant fibers as a mechanism of post-tetanic potentiation. *Exp Neurol* 49:736–749.
- Wallace C, Hawrylak N, Greenough WT (1991) Studies of synaptic structural modifications after long-term potentiation and kindling: context for a molecular morphology. In: *Long-term potentiation: a debate of current issues* (Baudry M, Davis JL, eds), pp 189–232. Cambridge, MA: MIT.
- Wenzel J, Lammert G, Meyer U, Krug M (1991) The influence of long-term potentiation on the spatial relationship between astrocyte processes and potentiated synapses in the dentate gyrus neuropil of rat brain. *Brain Res* 560:122–131.